

# Detection of Accelerator-Produced Neutrinos at a Distance of 250 km

S. H. Ahn<sup>h</sup>, S. An<sup>h</sup>, S. Aoki<sup>g</sup>, H. G. Berns<sup>t</sup>, H. C. Bhang<sup>o</sup>, S. Boyd<sup>t</sup>, D. Casper<sup>b</sup>, T. Chikamatsu<sup>f†</sup>, J. H. Choi<sup>c</sup>, S. Echigo<sup>g</sup>, M. Etoh<sup>q\*</sup>, K. Fujii<sup>g</sup>, S. Fukuda<sup>r</sup>, Y. Fukuda<sup>r</sup>, W. Gajewski<sup>b</sup>, U. Golebiewska<sup>s</sup>, T. Hara<sup>g</sup>, T. Hasegawa<sup>p</sup>, Y. Hayato<sup>f</sup>, J. Hill<sup>j</sup>, S. J. Hong<sup>h</sup>, M. Ieiri<sup>f</sup>, T. Inada<sup>n</sup>, T. Inagaki<sup>i</sup>, T. Ishida<sup>f</sup>, H. Ishii<sup>f</sup>, T. Ishii<sup>f</sup>, H. Ishino<sup>f‡</sup>, M. Ishitsuka<sup>r</sup>, Y. Itow<sup>r</sup>, T. Iwashita<sup>g</sup>, H. I. Jang<sup>c§</sup>, J. S. Jang<sup>c</sup>, E. J. Jeon<sup>f</sup>, E. M. Jeong<sup>c</sup>, C. K. Jung<sup>j</sup>, T. Kadowaki<sup>n</sup>, T. Kajita<sup>r</sup>, J. Kameda<sup>r</sup>, K. Kaneyuki<sup>r</sup>, I. Kato<sup>i</sup>, Y. Kato<sup>f</sup>, E. Kearns<sup>a</sup>, S. Kenmochi<sup>k</sup>, B. H. Khang<sup>o</sup>, A. Kibayashi<sup>e</sup>, D. Kielczewska<sup>s</sup>, B. J. Kim<sup>o</sup>, C. O. Kim<sup>h</sup>, H. I. Kim<sup>o</sup>, J. H. Kim<sup>o</sup>, J. Y. Kim<sup>c</sup>, S. B. Kim<sup>o</sup>, S. Kishi<sup>n</sup>, M. Kitamura<sup>g</sup>, K. Kobayashi<sup>r</sup>, T. Kobayashi<sup>f</sup>, Y. Kobayashi<sup>r</sup>, M. Kohama<sup>g</sup>, D. G. Koo<sup>h</sup>, Y. Koshio<sup>r</sup>, W. Kropp<sup>b</sup>, G. Kume<sup>g</sup>, E. Kusano<sup>f</sup>, J. G. Learned<sup>e</sup>, H. K. Lee<sup>c</sup>, J. W. Lee<sup>h</sup>, S. B. Lee<sup>f</sup>, I. T. Lim<sup>c</sup>, S. H. Lim<sup>c</sup>, H. Maesaka<sup>i</sup>, K. Martens<sup>j×</sup>, T. Maruyama<sup>pb</sup>, S. Matsuno<sup>e</sup>, C. Mauger<sup>j</sup>, C. McGrew<sup>j</sup>, M. Minakawa<sup>f</sup>, S. Mine<sup>b</sup>, M. Miura<sup>r</sup>, S. Miyamoto<sup>f</sup>, K. Miyano<sup>k</sup>, S. Moriyama<sup>r</sup>, S. Mukai<sup>i</sup>, M. Nakahata<sup>r</sup>, K. Nakamura<sup>f</sup>, M. Nakamura<sup>k</sup>, I. Nakano<sup>l</sup>, T. Nakaya<sup>i</sup>, S. Nakayama<sup>r</sup>, K. Nakayoshi<sup>f</sup>, K. Nishijima<sup>g</sup>, K. Nishikawa<sup>i</sup>, S. Nishiyama<sup>g</sup>, S. Noda<sup>g</sup>, H. Noumi<sup>f</sup>, Y. Obayashi<sup>r</sup>, J. K. Oh<sup>h</sup>, A. Okada<sup>r</sup>, M. Onchi<sup>g</sup>, T. Otaki<sup>g</sup>, Y. Oyama<sup>f</sup>, M. Y. Pac<sup>d</sup>, H. Park<sup>f</sup>, S. H. Park<sup>h</sup>, S. K. Park<sup>h</sup>, A. Sakai<sup>f</sup>, M. Sakuda<sup>f</sup>, N. Sakurai<sup>r</sup>, N. Sasao<sup>i</sup>, K. Sato<sup>g</sup>, K. Scholberg<sup>a#</sup>, E. Seo<sup>o</sup>, E. Sharkey<sup>j</sup>, K. Shiino<sup>f</sup>, A. Shima<sup>i</sup>, M. Shiozawa<sup>r</sup>, H. So<sup>o</sup>, H. Sobel<sup>b</sup>, A. Stachyra<sup>t</sup>, J. L. Stone<sup>a</sup>, L. R. Sulak<sup>a</sup>, A. Suzuki<sup>g</sup>, Y. Suzuki<sup>f</sup>, Y. Suzuki<sup>r</sup>, M. Takasaki<sup>f</sup>, M. Takatsuki<sup>g</sup>, K. Takenaka<sup>g</sup>, H. Takeuchi<sup>r</sup>, Y. Takeuchi<sup>r</sup>, N. Tamura<sup>k</sup>, K. H. Tanaka<sup>f</sup>, Y. Tanaka<sup>g</sup>, K. Tashiro<sup>g</sup>, K. Tauchi<sup>f</sup>, T. Toshito<sup>r</sup>, Y. Totsuka<sup>r</sup>, V. Tumakov<sup>f</sup>, T. Umeda<sup>l</sup>, M. Vagins<sup>b</sup>, C. W. Walter<sup>a</sup>, R. J. Wilkes<sup>t</sup>, S. Yamada<sup>r</sup>, T. Yamaguchi<sup>l</sup>, Y. Yamanoi<sup>f</sup>, C. Yanagisawa<sup>j</sup>, H. Yokoyama<sup>i</sup>, H. Yokoyama<sup>n</sup>, J. Yoo<sup>o</sup>, M. Yoshida<sup>m</sup>, S. Y. You<sup>c</sup>

<sup>a</sup>Department of Physics, Boston University, Boston, MA 02215

<sup>b</sup>Department of Physics and Astronomy, University of California, Irvine, Irvine, CA 92697-4575

<sup>c</sup>Department of Physics, Chonnam National University, Kwangju 500-757, KOREA

<sup>d</sup>Department of Physics, Dongshin University, Naju 520-714, KOREA

<sup>e</sup>Department of Physics and Astronomy, University of Hawaii, Honolulu, HI 96822

<sup>f</sup>Institute of Particle and Nuclear Studies, KEK, Tsukuba, Ibaraki 305-0801, JAPAN

<sup>g</sup>Kobe University, Kobe, Hyogo 657-8501, JAPAN

<sup>h</sup>Department of Physics, Korea University, Seoul 136-701, KOREA

<sup>i</sup>Department of Physics, Kyoto University, Kyoto 606-8502, JAPAN

<sup>j</sup>Department of Physics and Astronomy, State University of New York, Stony Brook, NY 11794-3800

<sup>k</sup>Department of Physics, Niigata University, Niigata, Niigata 950-2181, JAPAN

<sup>l</sup>Department of Physics, Okayama University, Okayama, Okayama 700-8530, JAPAN

<sup>m</sup>Department of Physics, Osaka University, Toyonaka, Osaka 560-0043, JAPAN

<sup>n</sup>Department of Physics, Science University of Tokyo, Noda, Chiba 278-0022, JAPAN

<sup>o</sup>Department of Physics, Seoul National University, Seoul 151-742, KOREA

<sup>p</sup>Research Center for Neutrino Science, Tohoku University, Sendai, Miyagi 980-8578, JAPAN

<sup>q</sup>Department of Physics, Tokai University, Hiratsuka, Kanagawa 259-1292, JAPAN

<sup>r</sup>Institute for Cosmic Ray Research, University of Tokyo, Kashiwa, Chiba 277-8582, JAPAN

<sup>s</sup>Institute of Experimental Physics, Warsaw University, 00-681 Warsaw, POLAND

<sup>t</sup>Department of Physics, University of Washington, Seattle, WA 98195-1560

<sup>†</sup>Present address: Miyagi Gakuin Women's College, Sendai, Miyagi 981-8557, JAPAN

<sup>\*</sup>Present address: Research Center for Neutrino Science, Tohoku University, Sendai, Miyagi 980-8578, JAPAN

<sup>‡</sup>Present address: Tokyo Institute of Technology, Tokyo 152-8550, JAPAN

<sup>§</sup>Present address: Department of Civil Engineering, Seokang College, Kwangju, 500-742, KOREA

<sup>×</sup>Present address: Department of Physics, University of Utah, Salt Lake City, UT 84112

<sup>‡</sup>Present address: Institute of Particle and Nuclear Studies, KEK, Tsukuba, Ibaraki 305-0801, JAPAN

<sup>#</sup>Present address: Department of Physics, Massachusetts Institute of Technology, Cambridge, MA 02139

(February 4, 2008)

The KEK to Kamioka long-baseline neutrino experiment (K2K) has begun its investigation of neutrino oscillations suggested by atmospheric neutrino observations. Twenty-eight neutrino events have been detected in coincidence with the expected arrival time of the beam in the 22.5 kt fiducial volume of Super-Kamiokande, the far detector at 250 km distance. The expectation is  $37.8^{+3.5}_{-3.8}$ , derived using measurements of neutrino interactions in a near detector and extrapolation using a beam simulation validated by a measurement of pion kinematics after production and focusing. The background is of order  $10^{-3}$  events.

PACS numbers: 14.60.Pq, 13.15.+g, 23.40.Bw, 95.55.Vj

The Standard Model of electroweak interactions has been tested with exceptional precision. The model, however, does not address the question of the origin of generations and their mixing. The existence of neutrino oscillations implies that neutrinos are massive and that lepton flavors are not conserved quantum numbers. It enables us to study relations between mass and flavor eigenstates in the lepton sector. Experiments on atmospheric neutrinos have found a significant deficit in the flux of  $\nu_\mu$  which have travelled an earth scale distance [1–3]. The interpretation of these results provides not only strong evidence of  $\nu_\mu \rightarrow \nu_\tau$  (or  $\nu_\mu \rightarrow \nu_{\text{sterile}}$ ) oscillations [4,5] but also evidence for different mixing properties in the lepton and quark sectors. For a neutrino energy  $E_\nu$  (GeV) and a distance from the source  $L$  (km), the oscillation probability can be written in terms of the mixing angle  $\theta$  and the difference of the squared masses  $\Delta m^2$  (eV<sup>2</sup>) in two flavor approximation as  $P(\nu_\mu \rightarrow \nu_x) = \sin^2 2\theta \sin^2(1.27 \Delta m^2 L / E_\nu)$ .

The KEK to Kamioka long-baseline neutrino experiment (K2K) is the first accelerator-based experiment with hundreds of km neutrino path length. The intense, nearly pure neutrino beam (98.2%  $\nu_\mu$ , 1.3%  $\nu_e$ , and 0.5%  $\bar{\nu}_\mu$ ) has an average  $L/E_\nu \approx 200$  ( $L = 250$  km,  $\langle E_\nu \rangle \approx 1.3$  GeV). The neutrino beam properties are measured just after production, and the kinematics of parent pions are measured *in situ* to extrapolate the measurements at the near detector to the expectation at the far detector. K2K focuses on the study of the existence of neutrino oscillations in  $\nu_\mu$  disappearance that is observed in atmospheric neutrinos, and on the search for  $\nu_\mu \rightarrow \nu_e$  oscillation with well understood flux and neutrino composition in the  $\Delta m^2 \geq 2 \times 10^{-3}$  eV<sup>2</sup> region. In this letter, the first results on the event rates with 100 days of data taken from June 1999 to June 2000 corresponding to  $2.29 \times 10^{19}$  protons on target, and the performance of the critical components of the long-baseline neutrino experiment are described.

The K2K neutrino beam [6,7] is a horn-focused wide band  $\nu_\mu$  beam. The primary beam for K2K is 12 GeV kinetic energy protons from the KEK proton-synchrotron (KEK-PS) [8]. Every 2.2 s, approximately  $6 \times 10^{12}$  protons in nine bunches are fast-extracted in a single turn, making a 1.1  $\mu$ s beam spill. These protons are focused onto a 30 mm diameter, 66 cm long aluminum target which is a current carrying element in the first of a pair of horn magnets operating at 250 kA [9]. This design maximizes the efficiency of the toroidal magnetic field to focus positive pions produced in proton-aluminum interactions, while sweeping out negative secondary particles.

Downstream of the horn system, before the 200 m long decay volume where the pions decay to  $\nu_\mu$  and muons, a gas-Cherenkov detector (PIMON) [10] is occasionally put in the beam to measure the kinematics of the pions after their production and subsequent focusing. After the decay volume, an iron and concrete beam dump stops

essentially all charged particles except muons with an energy greater than 5.5 GeV. Downstream of the dump there is a “muon monitor” (MUMON) [10] consisting of a segmented ionization chamber and an array of silicon pad detectors. This monitors the residual muons spill-by-spill to check beam centering and muon yield. The ionization chamber consists of 5 cm wide strips covering roughly  $2 \times 2$  m<sup>2</sup> area with separate planes for horizontal and vertical read-out. The 26 silicon pads, each of  $\sim 10$  cm<sup>2</sup> transverse area, are distributed through a  $3 \times 3$  m<sup>2</sup> area.

Neutrino interactions near the production site are measured by a set of detectors with complementary abilities. The detectors are located approximately 300 m from the pion production target with approximately 70 m of earth eliminating virtually all prompt beam products other than neutrinos. A one kiloton water Cherenkov detector (1kt) uses the same technology and analysis algorithms as the far detector, Super-Kamiokande (SK). It has 680 20” photomultiplier tubes (PMTs) on a 70 cm grid lining a 8.6m diameter, 8.6m high cylinder. The PMTs themselves and their arrangement are the same as in SK, giving the same fractional coverage by photo-cathode (40%). A scintillating fiber detector (SciFi) [11] with a 6 ton water target has tracking capability, and allows discrimination between different types of interactions such as quasi-elastic or inelastic. Downstream of the SciFi there is a lead glass array for tagging electromagnetic showers. A muon range detector (MRD) [12], measures the energy, angle, and production point of muons from charged current (CC)  $\nu_\mu$  interactions. It covers  $7.6 \times 7.6$  m<sup>2</sup> transverse area with four 10-cm iron plates, followed by eight 20-cm iron plates, all interleaved with drift tubes. The total mass is 915 tons. The 6632 drift tubes each has  $5 \times 7$  cm<sup>2</sup> cross section, and are arranged in horizontal and vertical read-out planes.

The far detector for K2K is the SK detector located in the Kamioka Observatory, Institute for Cosmic Ray Research (ICRR), University of Tokyo, which has been taking data since 1996. Its performance and results have been documented in the literature [4]. Event selection for this detector uses timing synchronization with the KEK-PS via the Global Positioning System (GPS) [13].

The beam-line was aligned by GPS position survey [6]. The precision of this survey for the line from the target to the far detector is better than 0.01 mr and the construction precision for the near site alignment is better than 0.1 mr. The predicted neutrino spectrum at 250 km is approximately the same over nearly 1 km, giving a required accuracy of 3mr for the pointing of the beam.

The steering and the monitoring of the  $\nu_\mu$  beam are carried out based on the MUMON measurement. The  $\nu_\mu$  and muons in the decay volume originate from the same pion decays, so the measured center position of the muon profile is correlated with the  $\nu_\mu$  beam direction. The r.m.s. muon profile width is  $\sim 90$  cm for both the horizontal and vertical directions. These measurements

are used in tuning the beam direction at the start of every beam period, usually once per month. Since there is a magnetic field in and around the target, the direction of the secondary pions, which determines the direction of decay  $\nu_\mu$  and muons, is sensitive to the position of the primary proton beam at the target. A 1 mm displacement of protons at the target face causes roughly 0.5 mr deflection to the opposite direction for muons observed by the MUMON [14]. During beam tuning, the primary proton position at the target is adjusted so that the muon profile is centered on the SK direction within 0.1 mr. The center of the muon profile is measured to be stable spill-by-spill within  $\pm 1$ mr in each dimension throughout the whole experimental period. The stability of the muon yield is directly related to the stability of the horn-focused  $\nu_\mu$  beam. The yield normalized to proton intensity measured by a current transformer is stable spill-by-spill within a measurement uncertainty of 2%.

The characteristics and stability of the  $\nu_\mu$  beam itself are directly monitored at the near site by the MRD using  $\nu_\mu$  interactions with iron. The large transverse area of MRD makes it possible to measure the beam direction and width (profile), and the large mass makes it possible to measure the time stability of the  $\nu_\mu$  event rate, profile and spectrum. The location of the center of the profile gives the beam direction. For the profile measurement, the starting point of a reconstructed muon track is regarded as the vertex of the  $\nu_\mu$ -iron interaction. The data reduction for the profile measurement requires: a) Only tracks around the time of the beam spill are accepted. b) Tracks with a common vertex are taken as a single event with the longest track assumed to be a muon. c) Muons entering or exiting the detector are rejected. d) Any muons with reconstructed energy lower than 0.5 GeV or higher than 2.5 GeV are rejected in order to avoid regions of small acceptance. The vertex distribution is corrected for geometrical acceptance to obtain the beam profile. As shown in Fig. 1(a), the horizontal profile is well centered on the SK direction. The profile width is well reproduced by the beam simulation which is described below. The profile center is plotted as a function of time in Fig. 1(b). The  $\nu_\mu$  direction has been stable within  $\pm 1$  mr throughout all data-taking periods. The vertical profile is also well centered on the SK direction and stable. For the event rate and kinematic distribution analyses no energy cut is made, but only events with vertices inside the fiducial volume defined by a cylinder of 3m radius in the upstream 9 iron plates are accepted. The measured rate of  $\nu_\mu$ -iron events is typically 0.05 events/spill and can be monitored on a daily basis with good statistics. The event rate normalized to proton intensity is stable within the statistical error of the MRD measurement. The muon energy and angular distributions are also continuously monitored. They show no change as a function of time, implying the  $\nu_\mu$  energy spectrum is stable throughout this period.

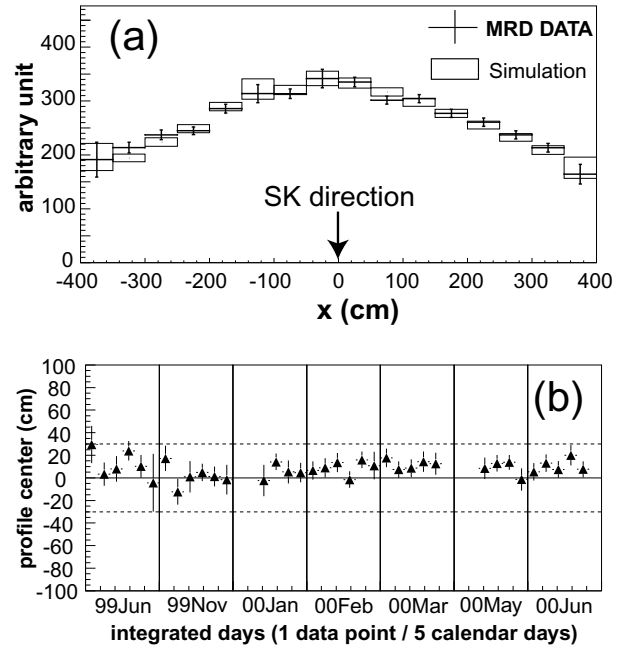


FIG. 1. (a) Horizontal profile of the  $\nu_\mu$  beam measured by MRD in a one month period (points with error bars), and simulated (boxes; size corresponds to error). Errors include statistics and uncertainty of the acceptance correction. The normalization is by the area under the histograms. (b) Stability of the  $\nu_\mu$  beam direction. The fitted center of the horizontal profile is plotted for five day periods, with error bars from the fits. The dashed lines show  $\pm 1$ mr directions to SK.

Comparison between expected and observed numbers of  $\nu_\mu$  events at the far site is done with this knowledge of measured beam stability. To predict the  $\nu_\mu$  beam characteristics at the far site, a normalization measurement at the near site and the extrapolation of the information from near to far are necessary. For the rate normalization, the 1kt is used so that any detector or analysis bias is suppressed. For the extrapolation, the beam simulation is used, which is validated by the PIMON measurement as described below. This simulation is based on GEANT [15] with detailed description of materials and magnetic fields in the target region and decay volume. It uses as input a measurement of the primary beam profile at the target. Primary proton interactions on aluminum are modeled with a parameterization of hadron production data [16]. Other hadronic interactions are treated by GEANT-CALOR [17].

Once the kinematic distribution of pions after production and focusing is known, it is possible to predict the  $\nu_\mu$  spectrum at any distance from the source. The pion momentum and angular distribution is measured by the PIMON. Cherenkov photons generated by pions in the detector are focused by a pie-shaped spherical mirror to an array of PMTs of 8 mm effective diameter in its focal plane. Photons emitted by particles with the same velocity and incident angle with respect to the mirror arrive at the same position in the focal plane. This is independent

of photon incident position with respect to the mirror. The photon distribution on the PMT array is a superposition of slices of the Cherenkov rings from particles of various velocities and angles. Measurements are made at seven indices of refraction, controlled by gas pressure, to give additional information on the velocity distribution of the particles. The indices of refraction are chosen so that the corresponding pion momentum interval is 400 MeV/c. The pion two-dimensional distribution of momentum versus angle is derived by unfolding the photon distribution data with various indices of refraction. The binning of extracted pion momentum and angular distributions are 1 GeV/c and 10 mr, respectively. To avoid background from 12 GeV primary protons, the index of refraction is adjusted below the Cherenkov threshold of 12 GeV protons ( $1 - \beta \approx 2.6 \times 10^{-3}$ ). As a consequence, analysis is done for  $P_\pi \geq 2\text{GeV}/c$ , giving the  $\nu_\mu$  energy spectral shape above 1 GeV. Figure 2 shows the inferred  $\nu_\mu$  energy spectral shape at the near site and the far to near  $\nu_\mu$  flux ratio along with the beam simulation result. The beam simulation is well validated by the PIMON measurement without any tuning.

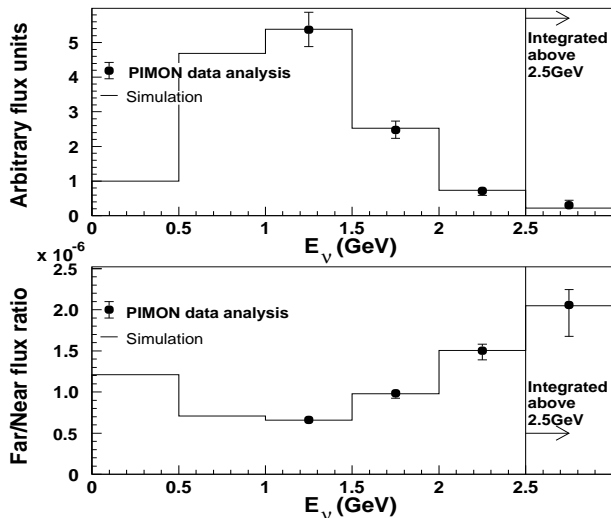


FIG. 2. The top figure shows the  $\nu_\mu$  energy spectral shape at the near site and the bottom figure shows the far to near  $\nu_\mu$  flux ratio. The histograms are from the beam simulation results. The data points are derived from the PIMON measurement. For the top figure, normalization is done by area above 1 GeV. The vertical error bars for the data points reflect the total uncertainty.

The  $\nu_\mu$  interaction rate at the near site is measured in the 1kt by detecting Cherenkov light emitted from produced charged particles. The vertices and directions of Cherenkov rings are reconstructed with the same methods as in SK [2]. In the 1kt, however, an analog sum of signals from all PMTs is recorded by an FADC to select beam spills with only one event. The definition of events per spill is the number of peaks of the FADC signal with  $> 1000$  collected photo-electrons (p.e.) ( $\approx 100\text{MeV}$

deposited energy). The average number of events observed in the full detector is about 0.2/spill including entering background events due to cosmic rays or  $\nu_\mu$  induced muons from upstream (about 1.5% of events in the fiducial volume defined below). Thus  $\geq 2$  events occur in about 10% of those spills with  $\geq 1$  event. Neutrino interactions are selected by requiring: a) There is no detector activity in the  $1.2\mu\text{s}$  preceding the beam spill. b) Only a single event is observed in the FADC peak search for that spill. c) The reconstructed vertex is inside the 25 t fiducial volume defined by a 2 m radius, 2 m long cylinder along the beam axis, in the upstream side of the detector. The detection efficiency of the 1kt detector for detecting CC interactions is 87% and for neutral current inelastic ( $\text{NC}_{\text{inel}}$ ) interactions it is 55%. The expected ratio of CC to  $\text{NC}_{\text{inel}}$  gives an overall efficiency of 72%. The main source of inefficiency is the 1000 p.e. threshold of the peak search in the FADC signal. The neutrino interaction simulator used for efficiency calculations is the same as that used in all SK analyses. Finally the number of  $\nu_\mu$  events in 1kt is corrected for spills with multiple events. The average  $\nu_\mu$  event rate per proton hitting the target is  $3.2 \times 10^{-15}$ . Correcting for efficiencies, relative target masses, and detector live times, the expected  $\nu_\mu$  signal at the far site is estimated by applying the extrapolation from the experimentally validated beam simulation.

Accelerator-produced neutrino interactions at the far site, SK, are selected by comparing two Universal Time Coordinated (UTC) time stamps from the GPS system,  $T_{\text{KEK}}$  for the KEK-PS beam spill start time and  $T_{\text{SK}}$  for the SK trigger time. The time difference between two UTC time stamps,  $\Delta(T) \equiv T_{\text{SK}} - T_{\text{KEK}} - \text{TOF}$  where  $\text{TOF}$  is the time of flight of a neutrino, should be distributed around the interval from 0 to  $1.1\mu\text{s}$  to match the width of the beam spill of the KEK-PS. Since the measured uncertainty of the synchronization accuracy for the two sites is  $< 200\text{ns}$ , beam-induced events are selected in a  $1.5\mu\text{s}$  window. Data reduction similar to that used in atmospheric neutrino analyses at SK [2,3] is applied to select fully contained (FC) neutrino interactions. The criteria are: a) There is no detector activity within 30  $\mu\text{s}$  before the event. b) The total collected p.e. in a 300 ns time window is  $> 200$  ( $\approx 20\text{MeV}$  deposited energy). c) The number of PMTs in the largest hit cluster in the outer-detector is  $< 10$ . d) The deposited energy is  $> 30\text{MeV}$ . Finally, a fiducial cut is applied accepting only events with fitted vertices inside the same 22.5kt volume used for SK atmospheric neutrino analysis. The detection efficiency of SK is 93% for CC interactions and 68% for  $\text{NC}_{\text{inel}}$  interactions, for a total of 79%. Similarly to the 1kt, the inefficiency is mainly due to the energy cut. Figure 3 shows the  $\Delta(T)$  distribution at various stages of the reduction. A clear peak in time with the neutrino beam from the KEK-PS is observed in the analysis time window. Twenty-eight FC events are observed in the fiducial volume. The arrival rate of neutrinos observed

by the far detector is consistent with constant within statistical fluctuation. The  $1.5\mu\text{s}$  selection window gives an expected background from atmospheric neutrino interactions of order  $10^{-3}$  events.

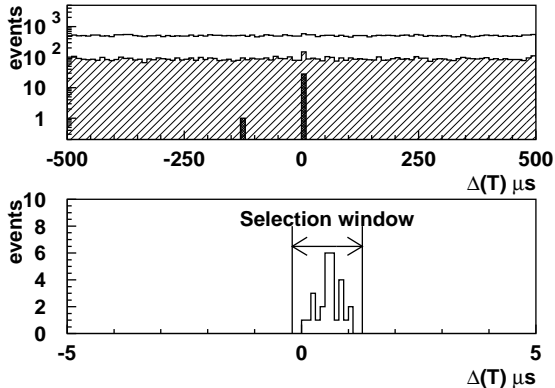


FIG. 3. Far site timing analysis: (top)  $\Delta(T)$  distribution over a  $\pm 500\mu\text{s}$  window for events remaining after cuts a) (unfilled histogram) and b) (hatched), and after all cuts except timing (shaded). The cuts are described in the text. (bottom)  $\Delta(T)$  for a  $\pm 5\mu\text{s}$  window for FC events with vertices in the fiducial volume.

The systematic uncertainty of the 1kt measurement is 5%, for which the leading terms are due to vertex fitting and its effect on the fiducial cut (4%), and the treatment of multiple events in a spill (3%). Other sources such as energy scale uncertainty are relatively small. The statistical uncertainty of the 1kt measurement is  $< 1\%$ . The systematic uncertainty of the extrapolation from the near site measurement is estimated to be  $^{+6}_{-7}\%$  based on the PIMON measurement uncertainty and beam simulation uncertainty for low energy neutrinos. The systematic uncertainty in the SK measurement is 3%, mainly due to the fiducial cut. The systematic uncertainty term coming from uncertainty in the neutrino energy spectrum and cross section is small due to cancellations. The quadrature sum of all known uncertainties for the far site event rate prediction is  $^{+9}_{-10}\%$ . The resulting expectation is  $37.8^{+3.5}_{-3.8}$  events in the absence of neutrino oscillations. The observed and expected numbers for various categories are summarized in Table I. The number of Cherenkov rings and particle identification are reconstructed by the same algorithms as those used at SK [2], and the event category definitions are also the same. The expected number of events for analyses of CC interactions in the other near detectors are  $41.0^{+6.0}_{-6.6}$  for MRD (iron target) and  $37.2^{+4.6}_{-5.0}$  for SciFi (water target) [18], each of which is consistent with the value based on 1kt analysis.

The crucial principles of K2K have been proven to work: The beam direction has been continuously monitored and controlled within  $\pm 1\text{mr}$  for several months duration by controlling the proton position on target

TABLE I. Summary of the observed and expected numbers of FC events in the fiducial volume at the far site.

Event Category	Observed	Expected
Single Ring $\mu$ -like	14	20.9
Single Ring $e$ -like	1	2.0
Multi Ring	13	14.9
TOTAL	28	$37.8^{+3.5}_{-3.8}$

with millimeter accuracy and operating the horn magnet stably. Pion kinematics have successfully been measured *in situ* allowing prediction of the neutrino beam at the distance of 250 km with six to seven percent accuracy. Events at the far site have been identified by means of GPS timing, reducing backgrounds to a negligible level. Twenty-eight FC neutrino events have been observed where  $37.8^{+3.5}_{-3.8}$  are expected. The experiment expects to accumulate  $10^{20}$  protons on target, providing sufficient statistics to study neutrino oscillations by spectral analysis for  $\nu_\mu$  disappearance.

We thank the KEK and ICRR Directorates for their strong support and encouragement. K2K is made possible by the inventiveness and the diligent efforts of the KEK-PS machine group. We gratefully acknowledge the cooperation of the Kamioka Mining and Smelting Company. This work has been supported by the Ministry of Education, Culture, Sports, Science and Technology, Government of Japan and its grants for Scientific Research, the Japan Society for Promotion of Science, the U.S. Department of Energy, the Korea Research Foundation, and the Korea Science and Engineering Foundation.

- [1] K.S.Hirata *et al.*, Phys. Lett. **B205**, 416 (1988); K.S.Hirata *et al.*, Phys. Lett. **B280**, 146 (1992); Y.Fukuda *et al.*, Phys. Lett. **B335**, 237 (1994); S.Hatakeyama *et al.*, Phys. Rev. Lett. **81**, 2016 (1998); Y.Fukuda *et al.*, Phys. Rev. Lett. **82**, 2644 (1999); Y.Fukuda *et al.*, Phys. Lett. **B467**, 185 (1999); D.Casper *et al.*, Phys. Rev. Lett. **66**, 2561 (1991); R.Becker-Szendy *et al.*, Phys. Rev. **D46**, 3720 (1992); W.W.M.Allison *et al.*, Phys. Lett. **B449**, 137 (1999); M.Ambrosio *et al.*, Phys. Lett. **B434**, 451 (1998).
- [2] Y.Fukuda *et al.*, Phys. Lett. **B433**, 9 (1998).
- [3] Y.Fukuda *et al.*, Phys. Lett. **B436**, 33 (1998).
- [4] Y.Fukuda *et al.*, Phys. Rev. Lett. **81**, 1562 (1998).
- [5] S.Fukuda *et al.*, Phys. Rev. Lett. **85**, 3999 (2000).
- [6] H.Noumi *et al.*, Nucl. Instr. and Meth. **A398**, 399 (1997).
- [7] M.Ieiri *et al.*, Proc. 1st Asian Particle Accelerator Conference (1998).
- [8] H. Sato, Proc. Particle Accelerator Conference (1999); K. Takayama, ICFA Beam Dynamics Newsletter No.20, (1999).

- [9] Y.Yamanoi *et al.*, Proc. 15th International Conference on Magnet Technology (1997); Y.Yamanoi *et al.*, IEEE Transactions on Applied Superconductivity **10**, 252 (2000); Y.Suzuki *et al.*, Proc. International Conference on Accelerator and Large Experimental Physics Control Systems (ICALEPCS) (1997); Proc. ICALEPCS (1999).
- [10] T.Maruyama, Ph.D. Thesis, Tohoku University (2000); K2K Beam Monitor Group, in preparation.
- [11] A.Suzuki *et al.*, Nucl. Instr. and Meth. **A453**, 165 (2000).
- [12] K2K MRD Group, submitted to Nucl. Instr. and Meth. **A**.
- [13] H.G.Berns and R.J.Wilkes, IEEE Nucl. Sci. **47**, 340 (2000).
- [14] H.Noumi *et al.*, in preparation.
- [15] R. Brun *et al.*, CERN DD/EE/84-1 (1987).
- [16] J.R.Sanford and C.L.Wang, BNL AGS internal reports No.BNL11299 and No.BNL11479 (1967); C.L.Wang, Phys. Rev. Lett. **25**, 1068 (1970); Y.Cho *et al.*, Phys. Rev. **D4**, 1967 (1971); J.G.Asbury *et al.*, Phys. Rev. **178**, 2086 (1969); G.J.Marmer *et al.*, Phys. Rev. **179**, 1294 (1969); G.J.Marmer and D.E.Lundquist, Phys. Rev. **D3**, 1089 (1971); J.V.Allaby *et al.*, CERN-TH-70-12 (1970).
- [17] T.A.Gabriel *et al.*, ORNL/TM-11185; C.Zeitnitz and T.A.Gabriel, Nucl. Instr. and Meth. **A349**, 106 (1994).
- [18] K2K Collaboration, in preparation.